ROLE OF MODEL PARTICLE SHAPE IN DISCRETE ELEMENT MODELS OF BED STRUCTURE IN CONTAINERS

MOHAMMAD HOSSEIN ABBASPOUR-FARD[1,2], BAGHER EMADI[1] and MEHDI KHOJASTEHPOUR[1]

[1]*Department of Agricultural Eng. (Farm Machinery)*
College of Agriculture
Ferdowsi University of Mashhad
Post Code: 9177948978, Mashhad, Iran

Accepted for Publication May 30, 2008

ABSTRACT

A container comprising 5,000 particles was simulated to investigate the role of particle shape on the bed structure of particulate materials. The effect of particle shape on the packing structure of granular beds was investigated in terms of bed height, the distribution of solid fraction, coordination number and the force acting at the bottom of the container. The solid fraction of the beds, which ranged from 0.7–0.9 for spherical particles and 0.6–0.8 for elongated particles, shows a compacted structure for beds of spherical particles. The average bed's solid fraction was 0.825 and 0.750 for beds of spherical and elongated particles, respectively. The overall reduction in the average solid fraction was about 8% as aspect ratio of particles changed from 1 to 4. The solid fraction frequency distribution of the beds implied a wider variety of void shape and size for elongated particles. There was also a significant difference between the coordination number of spherical particles and nonspherical particles. The coordination number was 4.7 and 3.6 for spherical and elongated particles, respectively. However, the change in the magnitude of coordination number was greater (15.1%) in between beds of spherical and nonspherical particles (particles of aspect ratio 2), than in between beds with aspect ratio 2 and 4 (11.3%). The numerical results indicated that for a reliable prediction of real material behavior via discrete element models, the employed model should be capable of manipulating individual elements with shape as close as possible to the shape of real particles.

[2] Corresponding author. TEL: +985118795620; FAX: +985118787430; EMAIL: abaspour@ferdowsi.um.ac.ir; Hossein_abbaspour@yahoo.co.uk

Journal of Food Process Engineering **33** (2010) 117–130.

DOI: 10.1111/j.1745-4530.2008.00322.x

PRACTICAL APPLICATIONS

As most of the agricultural materials comprise a system of individual nonspherical particles, a suitable discrete element (DE) model should be employed to gain realistic results. The DE models with spherical particles are very simple, which are less costly, while these models cannot predict the accurate behavior of systems comprising nonspherical particles. Hence, for such materials, using nonspherical models such as multisphere models is a must. Examples of such produce that need models with nonspherical or elongated elements are kernels and some fruits, whereas some other agricultural particles that are nearly spherical can be successfully simulated with DE models of spherical elements. The DE model employing the multisphere method (MSM) can be used for either case (spherical or nonspherical) to study the agricultural particulate materials processing operations on a particle scale (microscale), such as collision forces between individual grain and fruits that cannot easily be gained from experiments.

INTRODUCTION

Most agricultural produce, especially grains, have to be handled and stored for further processing operations. The majority of these operations involve particle flow. During the last few decades, several problems related to this matter have been studied experimentally and numerically. For example, flow from silos (Vibrascrew 1977; Tuzun and Nedderman 1979; Muhlhaus and Vardoulakis 1988; Wilcke *et al.* 1992; Ooi *et al.* 1998); flow pressure in silos (Ooms and Roberts 1985; Schmidt and Wu 1989; Bucklin *et al.* 1990); measurement of flow rates through orifices (Beverloo *et al.* 1961; Moysay and Lambert 1987); and the role of particle shape on particulate behavior on particle and bulk scales (Rothenburg and Bathurst 1992; Foutz and Thompson 1993; Cleary 1999; Jensen *et al.* 1999). The outcomes of these studies imply that the shape and size of particles are two inseparable parameters, which are needed for a satisfactory description of a particle's behavior in such operations. These two parameters can become more important in agricultural products as the shape and size of particles range from seeds, which may be less than a millimeter in diameter, to fruits whose dimensions can exceed tens of centimeters. Moreover, agricultural products have many shapes from round (approaching spheroid) to quite irregular in some seeds and fruits with a high aspect ratio.

In DE modeling (DEM), as an effective tool in this area, a particulate medium is represented by an assembly of discrete model particles. The shape of these particles is arbitrary, but it should ideally match the shape of actual

particles under consideration. The choice of particle shape representation is critical to the accuracy of the simulation of real particle behavior, the method used for contact detection and the method of computation of contact forces (Hogue 1998). Although contact detection and computation time are very important, the critical objective in DEM is the accurate simulation of the behavior of an assembly of real particles. The influence of particle shape on the predicted behavior is less well documented than the relationship between shape and the efficiency of contact detection (Favier *et al.* 1999).

For this reason, the application of the DEM to particular applications has resulted in various methods of particle shape representation. While the earliest DE models were two-dimensional and employed circular elements with linear contact models, later models have been developed with complex shape representation such as polygon (Krishnasamy and Jakiela 1995), ellipse (Ouadfel and Rothenburg 1999), and more recently the combination of primitives, mainly circle (Jensen *et al.* 1999) and sphere (Abbaspour-Fard 2001).

Attempts have also been made to describe and compare the shape of those particles deviating from a sphere. Beverloo *et al.* (1961) expressed the shape of some nonspherical seeds as a shape factor to study the influences of particle shape on the flow of different granular materials. Aspect ratio also has been frequently used to express the shape and compare nonspherical particles (Ng and Fang 1995; Ting *et al.* 1995; Hogue 1998; Cleary 1999).

In this study, a DE model based on the MSM of particle generation (Abbaspour-Fard 2001) has been used to investigate the effect of model particle shape on the prediction of the DE model for bed structure characteristics of particulate assemblies of different shapes. Aspect ratio has been selected as a criterion to compare and describe model particles of different shapes.

MATERIALS AND METHODS (SIMULATION PROCEDURE)

A flat-bottomed container 100 cm in width (50 times the diameter of a single sphere of unit radius) was simulated in two dimensions and the three-dimensional model particles were positioned in a single vertical layer. The height of the simulated box could be changed so that all model particles were generated in the container without any contact. Four sets of simulations were performed with identical particles of the same cross-sectional area (each particle comprised of a linear array of monosized spheres) and aspect ratios from 1 to 4. The total number of particles used in each set of simulation was 5,000, but with a different number of spheres per particle. The radius of monosized element spheres of a nonoverlapping multisphere model particle of aspect ratio n with an area equal to the area of a sphere of unit radius is

$$R_n = \left(\frac{1}{n}\right)^{\frac{1}{2}} \tag{1}$$

where n is the aspect ratio or the number of nonoverlapping element spheres in the model particle. These particles are shown in Fig. 1 and were used to simulate the beds of particulate materials shown in Fig. 2.

In each simulation, monosized (spherical and nonspherical) particles were placed into the container in a vertical layer without any contact (an array of singulated particles). In the case of nonspherical particles, a random

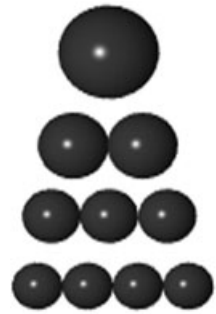

FIG. 1. PARTICLES USED IN THE SIMULATIONS WITH THE SAME CROSS-SECTION AREA BUT DIFFERENT ASPECT RATIO, RANGING FROM 1 TO 4

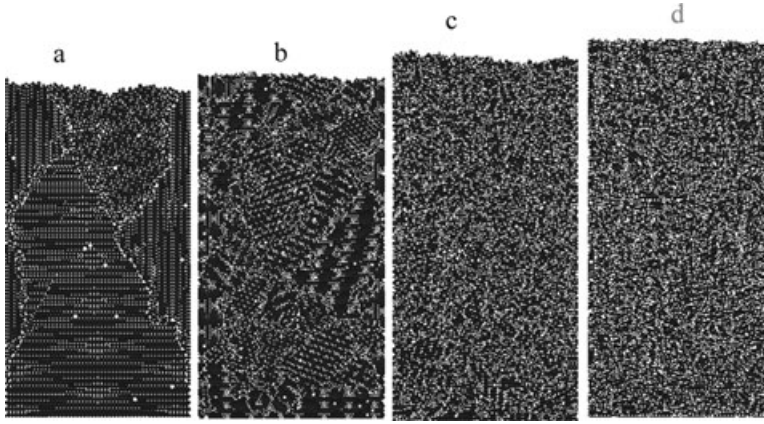

FIG. 2. BED HEIGHT AND STRUCTURE AT THE END OF CONSOLIDATION FOR PARTICLES THAT ARE SHOWN IN THE PREVIOUS FIGURE, HAVING AN ASPECT RATIO OF (a) 1, (b) 2, (c) 3 AND (d) 4

TABLE 1.
MODEL PARAMETER VALUES

Elastic modulus (GPa)	3.5
Poisson's ratio	0.3
Radius of the equivalent single sphere (cm)	1.0
Damping coefficient	0.5
Coefficient of friction (particle–particle)	0.2
Coefficient of friction (particle–wall)	0.5
Particle density (g/cm^3)	2.65
Time step (μs)	10
Number of particles	5,000

orientation was given to each particle in the x–z plane (vertical plane) in order to generate random packing of particles. Particles were then allowed to consolidate under a gravity field until particle movement was negligible. The relevant particle properties and computational conditions used in the simulations are shown in Table 1 (Abbaspour-Fard 2001). The simulations were performed using a noncommercial DEM code provided by Abbaspour-Fard (2001). The code was written in FORTRAN90, which was based on the MSM of particle generation and manipulation. This model was previously validated for some common phenomena in agricultural particulate materials processing such as Friction (scratching, sliding, rotation and particle collision). The validity of this model with MSM for the previously mentioned phenomena was examined by comparing the prediction of the model with the results of analytical calculations and experimental measurements. The details of model validation can be found in Abbaspour-Fard (2004).

RESULTS AND DISCUSSION

Bed Height and Distribution of Solid Fraction

The effect of particle shape on the prediction of the DE model for packing structure of particle beds (the arrangement of particles) at the end of consolidation was investigated by comparing the results of simulations in terms of bed height, the distribution of solid fraction through the bed, the force acting at the bottom of the container and particle coordination number. The results of the model for consolidated bed height and the bed structure for the assemblies of particles comprising aspect ratio from 1 to 4 are shown in Fig. 2. The bed height increased as the particle aspect ratio became higher because of greater void space between the particles of higher aspect ratio.

During consolidation, nonspherical particles moved downwards differently from spherical particles. These particles can create voids with different

shapes and sizes if the orientation of the adjacent particles is changed. This resulted in a more randomized and more porous structure which in turn led to a bed of greater height. It is seen that while the spherical particles could slide against each other to occupy the space between the particles, this could not happen for the elongated particles and some relatively large voids have been created due to randomized orientation of the particles. The relative position and randomized orientation of particles in the beds resulted in a more porous structure for beds with particles of higher aspect ratio and dissimilar particle bed configuration (general shape of the consolidated bed) for each assembly. Moreover, as reported by Abbaspour-Fard (2001), the nonspherical or elongated particles, comprised of monosized element spheres, may exhibit additional frictional effects than spherical particles, which was called pseudo-friction. This effect can also be the probable source of more porous structure in the bed of nonspherical particles. In the bed of spherical particles, some localized densely packed areas of homogenous particle packing structure have been observed, separated by narrow regions of higher porosity caused by bridging of particles. Dobry and Ng (1992) also noted that random arrays of identical spheres tend to crystallize in regular patterns. The size of the homogenous densely packed area was increasingly smaller in beds of particles of higher aspect ratio. There was a greater difference in the size of the area of densely packed particles in between beds with particles of aspect ratio 1 and 2 (comparing Fig. 2a,b) than in between beds with particles of aspect ratio 2 and 3 and from 3 to 4 (comparing Fig. 2c,d). This suggests that the change of particle shape from spherical to nonspherical had a greater effect on the packing structure of the particle bed in comparison with an increase in the aspect ratio of nonspherical particles.

The packing structure has been quantified by calculation of the solid fraction of the bed. The effect of the particle aspect ratio on the packing structure of the particle bed has been investigated by comparing the distribution of the solid fraction and the average solid fraction for the consolidated bed. The distribution of the solid fraction through the bed has been calculated by partitioning the particle bed into a grid of squares (mesh), each of which is 10×10 cm, so that in each square, a proper number of particles could be occupied (approximately 20 particles). The solid fraction for each square has been calculated from the number of particles, which their centroid located inside the square, and the area of the square. Figures 3–5 show the solid fraction distribution of the particle bed inside the container, the frequency distribution of solid fraction for particle beds with different aspect ratio and the average solid fraction for each, respectively. In Fig. 3, a lower solid fraction near the free surface has been seen for all particle beds, indicating a looser layer of particles in that region because of the lack of overburden.

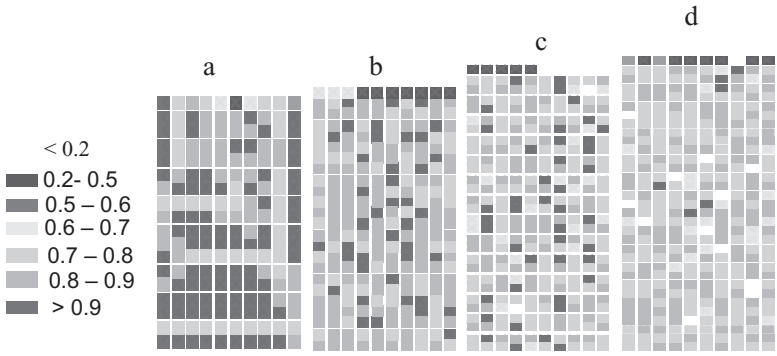

FIG. 3. DISTRIBUTION OF SOLID FRACTION IN THE CONTAINER FOR THE CONSOLIDATED ASSEMBLIES OF ASPECT RATIO OF (a) 1, (b) 2, (c) 3 AND (d) 4

The frequency distribution of solid fraction, which is characterized by skewness and kurtosis, is a particular parameter if the assumption is made that in a normal distribution of the solid fraction, there is a wide variety of voids that are different in shape and size in the bed. A distribution is negatively skewed when the curve shifts to the right side compared to a normal distribution. A distribution with a higher positive kurtosis means the distribution has more concentration around the mean. Table 2 shows the skewness and kurtosis of the curves in Fig. 4. It is shown that as the aspect ratio of bed's particles increased, a lower skewness and higher kurtosis was achieved, indicating a closer distribution to a normal distribution for these beds. This implies a wider variety of void shape and size in the bed. In contrast, the highly negative skew for the bed of spherical particles indicates a more uniform distribution of solid fraction for this bed, showing a smaller variation in void size and shape. In this bed, the frequency for solid fraction band of 0.5 shows the narrow regions of higher porosity caused by the bridging of particles that separated the densely packed areas. In the assemblies of particles with aspect ratio 2 and 3, the solid fraction distributed over a wider range (0.25–0.5). This indicates that the regions of higher porosity between the localized areas increased, which leads to a lower average solid fraction through the bed.

The average solid fraction decreased slightly as the aspect ratio increased from 1 to 2 and then decreased sharply as the aspect ratio increased further (as shown in Fig. 5). The overall reduction in the average solid fraction was about 8% as the bed particle aspect ratio changed from 1 to 4; however, most of this reduction occurred in between aspect ratio of 2 and 4.

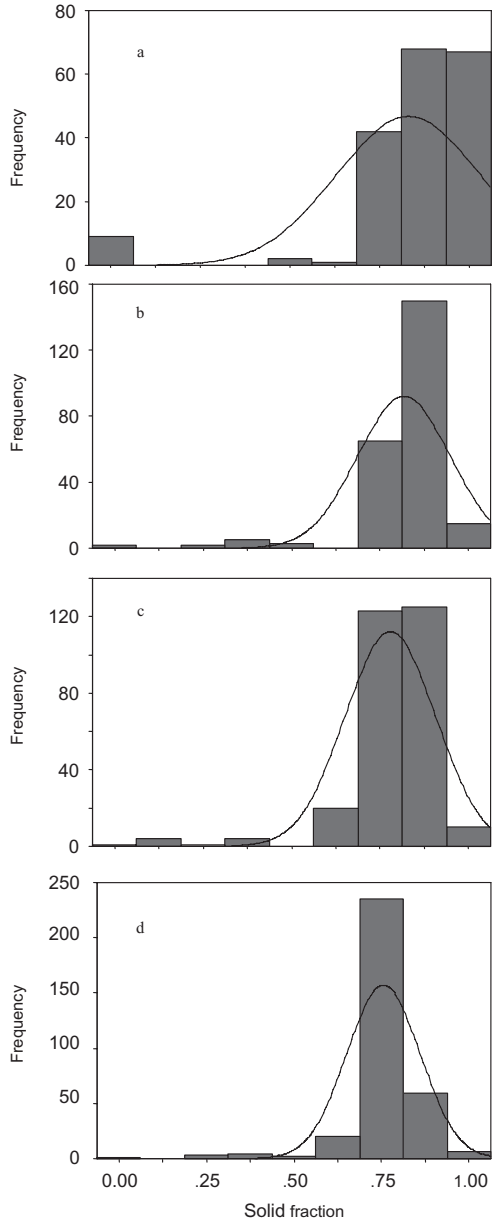

FIG. 4. FREQUENCY DISTRIBUTION OF SOLID FRACTION IN DIFFERENT PARTICLE ASSEMBLIES WITH ASPECT RATIO: (a) 1, (b) 2, (c) 3 AND (d) 4

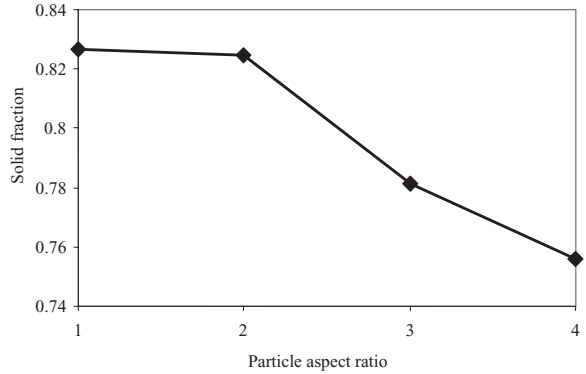

FIG. 5. RELATIONSHIP BETWEEN THE AVERAGE SOLID FRACTION OF THE PARTICLE BED AND ASPECT RATIO OF PARTICLES AT THE END OF CONSOLIDATION

TABLE 2.
SOME DESCRIPTIVE STATISTICS OF THE FREQUENCY DISTRIBUTION OF SOLID FRACTION FOR DIFFERENT PARTICLE ASSEMBLIES

Aspect ratio	Skewness	Kurtosis
1	–3.20	9.95
2	–3.09	12.34
3	–2.28	12.59
4	–2.69	13.16

Coordination Number

Coordination number is defined as the average number of contact points per particle in the particulate assembly. This parameter correlates with the degree of dilation of the bed, and it can be used as an index for comparison of particle bed structure. For a particulate assembly comprising spherical or elliptical particles, contact between particles can always be considered *point contact*. In assemblies of rod-like particles (e.g., cylindrical particles) in addition to point contact, contact may also occur along a line. In the case of particles with plane faces, contact may also occur over an area. In these simulations, any number of contacts between the element spheres of two neighboring particles has been considered as a *single* contact point.

Figure 6a shows the prediction of the DE model for the evolution of coordination number during consolidation of the beds with different aspect ratios. The consolidation started with no contact between particles ($C_n = 0$) and increased as the particles consolidated in the container. A constant C_n obtained

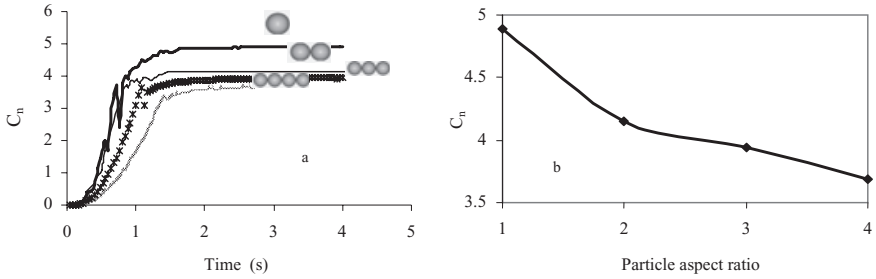

FIG. 6. (a) CHANGE IN COORDINATION NUMBER (C_n) DURING CONSOLIDATION OF BEDS WITH DIFFERENT ASPECT RATIO, AND (b) COORDINATION NUMBER FOR THE CONSOLIDATED PARTICLE ASSEMBLIES

for the particle bed indicated a stable assembly of particles. Despite different original bed height (particle generation stage) and different trends for the evolution of coordination number during consolidation, a stable condition was reached after almost 1.5 s for all beds. There was a significant difference between the coordination number of spherical particles (aspect ratio = 1) and nonspherical particles at the end of consolidation. Figure 6b shows the final coordination number for particle beds with different aspect ratios at the end of consolidation. The final coordination number of the beds generally decreased as the aspect ratio became higher, indicating a looser packing structure for nonspherical particles. The change in the magnitude of coordination number was greater (15.1%) between beds of particles with aspect ratios of 1 and 2 (spherical and nonspherical) than between beds of particles with aspect ratios of 2 and 4 (11.3%).

Force Acting at the Bottom of the Container

As noted, the consolidation step has been simulated for a condition of using normal gravitational acceleration and the weight of the particle assembly was identical for all assemblies. Therefore, any difference between the magnitudes of force acting at the bottom of the container for particle beds with a different aspect ratio might be because of the relative position of particles in the bed (bed structure). The sum of forces acting at the bottom of the container at the end of consolidation has been recorded and plotted against particle aspect ratio, as shown in Fig. 7. For all particle beds, it is seen that the calculated force between the particle bed and the bottom of the container was close to the actual weight of the particles. The difference for the bed of spheres was not considerable, i.e., 0.02% of actual weight. This difference increased to a maximum of 1.25% of actual weight for the particle bed of aspect ratio 2,

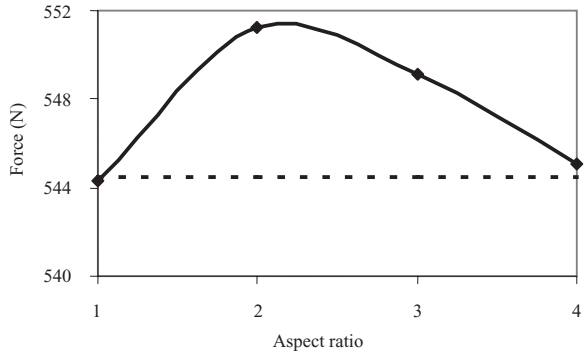

FIG. 7. TOTAL FORCE ACTING ON THE BOTTOM OF THE CONTAINER FOR PARTICLE ASSEMBLIES WITH DIFFERENT ASPECT RATIO; THE DASHED LINE SHOWS THE ACTUAL WEIGHT OF ASSEMBLIES

then decreased as the aspect ratio increased. In a normal gravitational condition, the total weight acting at the bottom of the container should be the same for all beds. The variation in the total contact force between particles and the container bottom for particles with different aspect ratio can be related to the number of contact points with the bottom. The damping forces calculated at each contact point and the fact that in a DE model, even in a quasi-static condition, the model particles are not *at rest* (vibrating particles). When the aspect ratio changed from 1 to 2, there were two element-spheres for each particle, but there was not a considerable change in the bed structure and solid fraction (Fig. 2a,b). So more contact points have been found between particles and the bottom (five more contact points than spherical particles). Because the damping acts on the contact points of the element sphere of a particle for a multisphere particle (see Abbaspour-Fard 2001), increasing the number of coincident contact points increases the damping. Moreover, as the particles were vibrating in the bed, the relative position and the relative velocity of the contacting spheres have been changed. It results in the total damping force between the particles, and the bottom of the container has been changed in an oscillating manner. The record of total damping force between the particles and the bottom of the container showed the maximum total damping force for the bed with spherical particles was 0.4% of the total weight of particles, while for the bed of comprising particles with an aspect ratio of 2, the maximum damping force was 1.05%. Therefore, it is concluded that the higher contact force for the particle bed of an aspect ratio of 2 was caused by the higher total damping force between particles and the container bottom. More numerical experiments are needed to normalize the damping force according to the number of concurrent contact points of particles.

CONCLUSION

The assembly of particles with different aspect ratios in a flat-bottomed container was performed employing a discrete element model with an MSM. A semi-two-dimensional container was prepared by using three-dimensional particles in a vertical layer. Particulate assemblies comprising particles with different aspect ratios ranging from 1 to 4 were created using some nonoverlapping spheres in order to investigate the effect of particle shapes on bed structure and flow characteristics of particles.

There was a distribution of solid fraction within each bed, with the closest distribution to the normal distribution for the beds of elongated particles. The localized densely packed areas have been separated by voids caused by the bridging of particles in the beds. It has also been observed that variation in bed structure and coordination number between beds of spherical particles with aspect ratio 1 (A.R. = 1) and nonspherical particles (A.R. = 2) were much greater than those between elongated particles (A.R. $\geq$ 2). This implies that to predict a realistic behavior of nonspherical particles, the DE models must be able to create a model particle's shape as closely as possible to the shape of the real materials. It can, therefore, be concluded that the results obtained from discrete element models with spherical elements cannot be generalized to real material comprising nonspherical particles. In this regard, the MSM model has the capability of generating both spherical and nonspherical elements with convex outer boundaries, which is matched to the outer surface of most agricultural produce.

REFERENCES

ABBASPOUR-FARD, M.H. 2001. Discrete element modelling of the dynamic behaviour of non-spherical particulate materials. PhD Thesis, Newcastle University, Newcastle upon Tyne, UK.

ABBASPOUR-FARD, M.H. 2004. Theoretical validation of a multi-sphere, discrete element model suitable for biomaterials handling simulation. Biosyst. Eng. *88*, 153–161.

BEVERLOO, W.A., LENIGER, H.A. and VAN DE VELDE, J. 1961. The flow of granular solids through orifices. Eng. Sci. *15*, 260–269.

BUCKLIN, R.A., THOMPSON, S.A. and ROSS, I.J. 1990. Bin-wall failure caused by eccentric discharge of free-flowing grain. J. Struct. Eng. *116*, 3173–3190.

CLEARY, P.W. 1999. The effect of particle shape on hopper discharge. *Second International Conference on CFD in the Minerals and Process Industries*, CSIRO, Melbourne.

DOBRY, R. and NG, T.T. 1992. Discrete modeling of stress-strain behavior of granular media at small and large strains. Eng. Comput. *9*, 129–143.

FAVIER, J.F., ABBASPOUR-FARD, M.H., KREMMER, M. and RAJI, A.O. 1999. Shape representation of axi-symmetrical, non-spherical particles in discrete simulations using multi-element model particles. Eng. Comput. *16*, 467–480.

FOUTZ, T.L. and THOMPSON, S.A. 1993. Comparison of loading response of packed grain and individual kernel. Trans. ASAE *36*, 569–576.

HOGUE, C. 1998. Shape representation and contact detection for discrete element simulations of arbitrary geometries. Eng. Comput. *15*, 374–390.

JENSEN, R.P., BOSSCHER, P., PLESHA, M.E. and EDIL, T.B. 1999. DEM simulation of granular media-structure interface: effect of surface roughness and particle shape. Int. J. Numer. Anal. Methods Geomech. *23*, 531–547.

KRISHNASAMY, J. and JAKIELA, M.S. 1995. A method to resolve ambiguities in corner–corner interactions between polygons in the context of motion simulation. Eng. Comput. *12*, 135–145.

MOYSAY, E.B. and LAMBERT, E.W. 1987. Flow rates of grains and oilseeds through orifices. *Particulate and Multiphase Processes*. Hemisphere Publi. Corp., Miami, FL.

MUHLHAUS, H.B. and VARDOULAKIS, I. 1988. The thickness of shear bands in granular materials. Geotechnique *37*, 271–283.

NG, T.T. and FANG, H.E. 1995. Cyclic behaviour of arrays of ellipsoids with different particles shape. ASME Appl. Mech. *201*, 59–71.

OOI, J.Y., CHEN, J.F. and ROTTER, J. 1998. Measurement of solids flow patterns in a gypsum silo. Powder Technol. *99*, 272–284.

OOMS, M. and ROBERTS, A.W. 1985. Reduction and control of flow pressures in cracked grain silo. Bulk Solids Handl. *5*, 1009–1016.

OUADFEL, H. and ROTHENBURG, L. 1999. An algorithm for detecting inter-ellipsoid contacts. Comput. Geotech. *24*, 245–263.

ROTHENBURG, L. and BATHURST, R.J. 1992. Micromechanical features of granular assemblies with planar elliptical particles. Geotechnique *42*, 79–95.

SCHMIDT, L.C. and WU, Y.H. 1989. Prediction of dynamic wall pressure on silos. Bulk Solids Handl. *9*, 333–338.

TING, J., MEACHUM, L.R. and ROWELL, J.D. 1995. Effect of particle shape on the strength and deformation mechanism of ellipse shape granular assemblies. Eng. Comput. *12*, 99–108.

TUZUN, U. and NEDDERMAN, R.M. 1979. Experimental evidence supporting kinematic modelling of the flow of granular media in the absence of drag. Power Technol. *24*, 257–266.

VIBRASCREW, I.T.N. 1977. Improving material flow from bin. Chem. Eng. Prog. *33*, 82–86.

WILCKE, W., CHANG, C.S. and HETZEL, G.H. 1992. Grain flow through guarded horizontal orifices. Appl Eng. Agric. *8*, 65–75.